A Basal Dromaeosaurid and Size Evolution Preceding Avian Flight

Alan H. Turner *et al.*

Science **317**, 1378 (2007);
DOI: 10.1126/science.1144066

data exhibit a complex structure suggestive of two-center quantum interferences. These rapid electronic dynamics will be an interesting topic for further study.

In the future, this work can be extended to a range of atomic and molecular systems to explore complex, correlated electron dynamics and highly excited states. Interesting topics such as the attosecond dynamics of electron transitions, the observation of ultrafast electron transfer in molecules, and the influence of molecular structure on these x-ray driven dynamics are challenging problems that are now accessible with the use of the techniques illustrated here.

References and Notes

1. A. H. Zewail, *Science* **242**, 1645 (1988).
2. O. Geßner *et al*., *Science* **311**, 219 (2006).
3. A. M. Rijs, M. H. M. Janssen, E. T. H. Chrysostom, C. C. Hayden, *Phys. Rev. Lett.* **92**, 123002 (2004).
4. M. H. Kim, L. Shen, H. Tao, T. J. Martinez, A. G. Suits, *Science* **315**, 1561 (2007).
5. A. Stolow, A. E. Bragg, D. M. Neumark, *Chem. Rev.* **104**, 1719 (2004).
6. S. Zamith *et al*., *J. Chem. Phys.* **119**, 3763 (2003).
7. R. R. Meier, *Space Sci. Rev.* **58**, 1 (1991).
8. H. Imanaka, M. A. Smith, *Geophys. Res. Lett.* **34**, L02204 (2007).
9. U. Becker, D. A. Shirley, Eds., *VUV and Soft X-Ray Photoionisation* (Plenum, New York, 1996).
10. H. C. Kapteyn, M. M. Murnane, I. P. Christov, *Phys. Today* **58**, 39 (2005).
11. Y. Hatano, *Phys. Rep.* **313**, 109 (1999).
12. A. Scrinzi, M. Y. Ivanov, R. Kienberger, D. M. Villeneuve, *J. Phys. B At. Mol. Opt. Phys.* **39**, R1 (2006).
13. M. Uiberacker *et al*., *Nature* **446**, 627 (2007).
14. L. Nugent-Glandorf *et al*., *Phys. Rev. Lett.* **8719**, 193002 (2001).
15. N. L. Wagner *et al*., *Proc. Natl. Acad. Sci. U.S.A.* **103**, 13279 (2006).
16. L. Miaja-Avila *et al*., *Phys. Rev. Lett.* **97**, 113604 (2006).
17. J. Ullrich *et al*., *Rep. Prog. Phys.* **66**, 1463 (2003).
18. A. S. Alnaser *et al*., *Phys. Rev. Lett.* **93**, 113003 (2004).
19. T. Weber *et al*., *Nature* **431**, 437 (2004).
20. H. D. Cohen, U. Fano, *Phys. Rev.* **150**, 30 (1966).
21. A. Rundquist *et al*., *Science* **280**, 1412 (1998).
22. S. Krummacher, V. Schmidt, F. Wuilleumier, *J. Phys. B At. Mol. Opt. Phys.* **13**, 3993 (1980).
23. Using 43.2-eV photons from a synchrotron, the partial cross section for inner-valence ionized states between 23 and 43 eV was measured to be 33% of the total photoionzation cross section (*22*).
24. T. Aoto *et al*., *J. Chem. Phys.* **124**, 234306 (2006).
25. J. H. D. Eland, E. J. Duerr, *Chem. Phys.* **229**, 13 (1998).
26. P. Baltzer, M. Larsson, K. Karlsson, B. Wannberg, M. C. Gothe, *Phys. Rev. A* **46**, 5545 (1992).
27. Some examples of such dissociation limits are (N, N^+) = (^3P, $^2P_0$), (^1S, $^4S_0$), (^1D,$^2D_0$), and (^1D, $^2P_0$).
28. This strong feature is probably due to the concentration of the $^2\Sigma_g^+$ oscillator strength in the region ranging from 27 to 31 eV (F-band). Dissociation from this band gives rise to a quasi-monoenergetic photoelectron peak, with a corresponding well-defined KER. The observed electron-energy width results from the soft x-ray pulse bandwidth.
29. We identify and distinguish bound and dissociative channels in the supporting online material. The triple coincidence data presented in fig. S1 confirms that we selectively probed highly excited dissociative states near the double-ionization threshold of N_2.
30. M. Lundqvist, D. Edvardsson, P. Baltzer, B. Wannberg, *J. Phys. B At. Mol. Opt. Phys.* **29**, 1489 (1996).
31. H. Sambe, D. E. Ramaker, *Chem. Phys.* **107**, 351 (1986).
32. D. Dill, J. L. Dehmer, *J. Chem. Phys.* **61**, 692 (1974).

33. We thank A. Czasch, T. Jahnke, A. Paul, W. Li, and B. Walker for technical support and useful discussions. We acknowledge support for this work from the NSF through the Physics Frontiers Centers Program and from the Department of Energy, Office of Science. This work made use of facilities provided by the NSF Engineering Research Center on Extreme Ultraviolet Science and Technology.

Supporting Online Material

www.sciencemag.org/cgi/content/full/317/5843/1374/DC1
SOM Text
Fig. S1
References

10 May 2007; accepted 23 July 2007
10.1126/science.1144920

A Basal Dromaeosaurid and Size Evolution Preceding Avian Flight

Alan H. Turner,[1]* Diego Pol,[2] Julia A. Clarke,[3,4,1] Gregory M. Erickson,[5] Mark A. Norell[1]

Fossil evidence for changes in dinosaurs near the lineage leading to birds and the origin of flight has been sparse. A dinosaur from Mongolia represents the basal divergence within Dromaeosauridae. The taxon's small body size and phylogenetic position imply that extreme miniaturization was ancestral for Paraves (the clade including Avialae, Troodontidae, and Dromaeosauridae), phylogenetically earlier than where flight evolution is strongly inferred. In contrast to the sustained small body sizes among avialans throughout the Cretaceous Period, the two dinosaurian lineages most closely related to birds, dromaeosaurids and troodontids, underwent four independent events of gigantism, and in some lineages size increased by nearly three orders of magnitude. Thus, change in theropod body size leading to flight's origin was not unidirectional.

Which nonflying maniraptoran dinosaurs are the closest relatives to birds (Avialae) has been debated (*1*–*5*). Dromaeosaurids and troodontids are the two clades consistently found to be most closely related to avialans (*1*–*8*). Discoveries of these dinosaurs, which illuminate the features ancestrally present in the first flighted theropods, have remained rare. Here we report a basal dromaeosaurid theropod: Theropoda Marsh, 1884; Maniraptora Gauthier, 1986; Paraves Sereno, 1997; Dromaeosauridae Matthew and Brown, 1922; *Mahakala omnogovae*, new taxon. The new taxon is small (~70 cm long) and possesses features absent in other dromaeosaurids but shared with early troodontids and avialans.

Holotype. Specimen number IGM (Mongolian Institute of Geology, Ulanbaatar) 100/1033, a partial skull and postcranial skeleton (Figs. 1 and 2).

Etymology. "Mahakala," Sanskrit for one of the eight protector deities (dharmapalas) in Tibetan Buddhism. The specific epithet refers to the southern Gobi provenance of this taxon.

Locality and horizon. The Tugrugyin Member of the Djadokhta Formation (Campanian) (*9*, *10*), Tugrugyin Shireh, Ömnögov, Mongolia (*10*, *11*).

Diagnosis. A small paravian diagnosed by the following combination of characters (autapomorphies are noted by *): a strongly compressed and anteroposteriorly broad ulna tapering posteriorly to a narrow edge*; an elongate lateral crest on the posterodistal part of the femur*; anterior caudal vertebrae with subhorizontal, laterally directed prezygapophyses*; a prominent supratrochanteric process; and the absence of a cuppedicus fossa.

Estimated at 70 cm long, *Mahakala* is similar in size to the basal avialan *Archaeopteryx* and basal members of other maniraptoran clades such as the oviraptorosaur *Caudipteryx* and the troodontid *Mei long*. The specimen is a young adult or near adult, based on the degree of neurocentral and astragalocalcaneal fusion, braincase coossification, and histological analysis (fig. S4). Thus, it can be distinguished from the contemporaneous *Archaeornithoides*, which is of similar size but is a juvenile (*12*).

The braincase, quadrate, and frontals are well preserved. Unlike dromaeosaurids but similar to troodontids such as *Sinovenator* (*7*) and *Mei* (*8*), the frontals are dorsoventrally vaulted and the interorbital region is narrow, indicating proportionally large orbits. The anterolateral corner of the frontal lacks the articulation notch present in other dromaeosaurids. The frontals transition smoothly from the orbital margin to the postorbital processes as in troodontids (*13*), but unlike the abrupt transition and sharply demarcated postorbital processes of dromaeosaurids. The supratemporal fossa margin is weakly curved, not sinuous as in all other dromaeosaurids except *Tsaagan* (*5*) and *Dromaeosaurus* [AMNH (American Museum of Natural History) FR

[1]Division of Paleontology, American Museum of Natural History, Central Park West at 79th Street, New York, NY 10024–5192, USA. [2]CONICET, Museo Paleontológico Egidio Feruglio, Avenida Fontana 140, (9100) Trelew, Argentina. [3]Department of Marine, Earth and Atmospheric Sciences, North Carolina State University, Campus Box 8208, Raleigh, NC 27695–8298, USA. [4]Division of Paleontology, North Carolina Museum of Natural Sciences, 11 West Jones Street, Raleigh, NC 27601–1029, USA. [5]Department of Biological Sciences, Florida State University, Dewey Street and Palmetto Drive, Tallahassee, FL 32306–1100, USA.

*To whom correspondence should be addressed. E-mail: turner@amnh.org

5356]. The quadrate is incipiently bistylic, unlike the single-headed ball-shaped process in other dromaeosaurids. A depression on the prootic may correspond to a secondary articulation surface for the quadrate. This depression corresponds topographically to the braincase articulation facet in birds and alvarezsaurids but is also present in the troodontid *Byronosaurus* (*14*). The lateral braincase wall lacks any indication of a well-developed otosphenoidal crest like that in troodontids (*14*). The paroccipital processes are relatively short and distally twisted rostrolaterally as in other dromaeosaurids.

The axis bears a single pneumatic opening and has small epipophyses that do not overhang the postzygapophyses. The sacrum comprises six apneumatic, coossified centra as in *Rahonavis* and mature specimens of *Velociraptor* (IGM 100/986 and IGM 100/985). The fused neural arches of the posterior sacral vertebrae form a bony lamina as in other dromaeosaurids. The tail is long as in basal avialans (such as *Archaeopteryx* and *Jeholornis*), basal troodontids (such as *Jinfengopteryx* and *Mei*), and other dromaeosaurids. The transition point occurs between caudals (Cd's) 11 and 12 and is more posteriorly located than in *Rahonavis* (proximal to Cd 9) or *Velociraptor* (proximal to Cd 10). The distal caudal postzygapophyses are smaller than the prezygapophyses. As in to other basal paravians, the postzygapophyses do not exceed the posterior margin of the vertebral centra. The lateral surface of the proximal caudals bears a low ridge similar

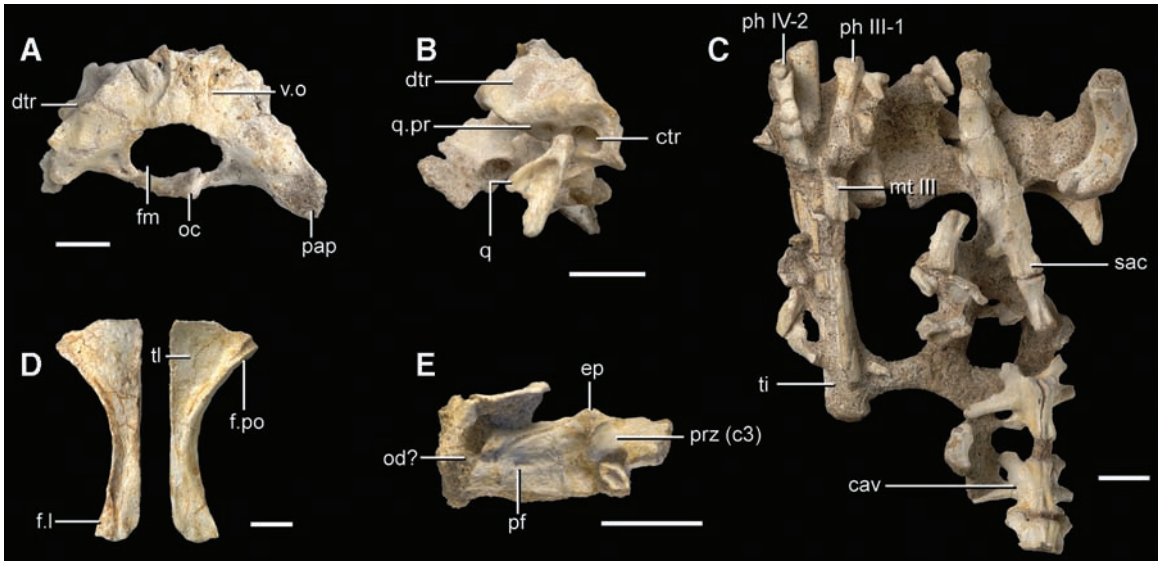

Fig. 1. *Mahakala omnogovae* IGM 100/1033, holotype. (**A**) Skull in occipital view. (**B**) Braincase in left lateral view. (**C**) Sacrum and partial right leg in ventral view. (**D**) Frontal in dorsal (left) and ventral (right) views. (**E**) Axis vertebra in left lateral view. Scale bars, 5 mm in (A), (B), (D), and E) and 1 cm in (C). Abbreviations are as follows: cav, caudal vertebra; ctr, caudal tympanic recess; dtr, dorsal tympanic recess; ep, epipophysis; f.l, lacrimal facet; f.po, postorbital facet; fm, foramen magnum; mt, metatarsus; oc, occipital condyle; od, odontoid; pap, paroccipital process; pf, pneumatic foramen; ph, phalanx; prz, prezygapophysis; q.pr, contact surface on prootic for quadrate; q, quadrate; ti, tibia; tl, tectal lobe; sac, sacrum; v.o, occipital vein track.

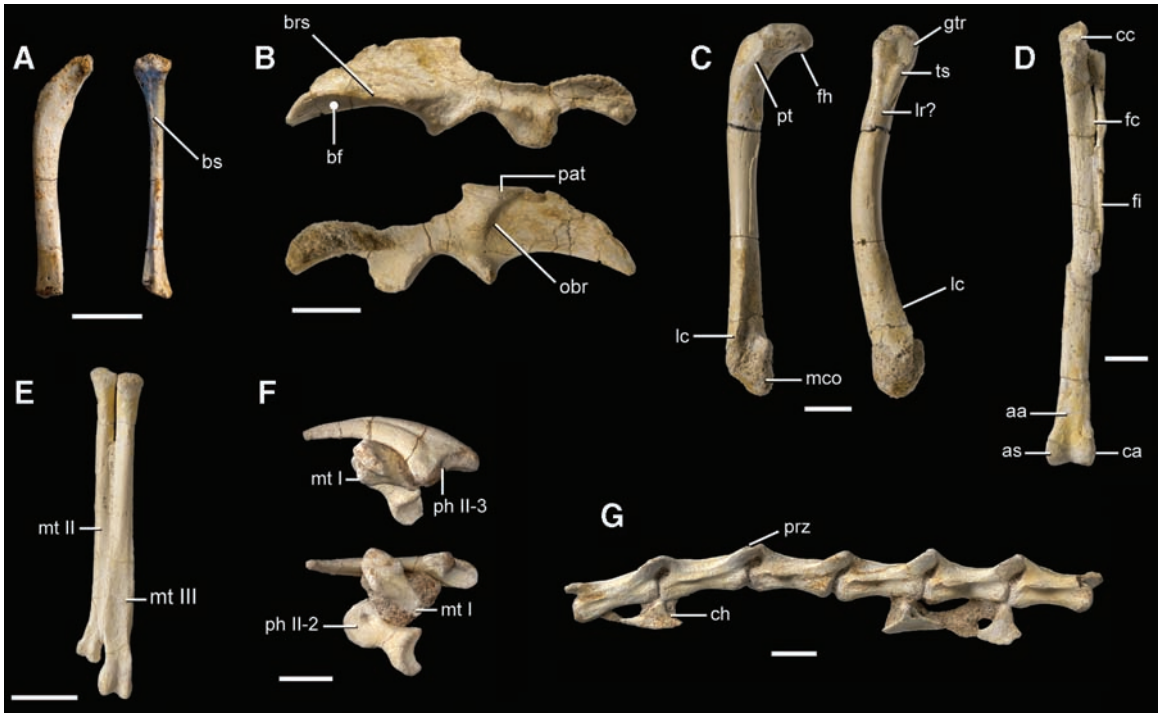

Fig. 2. *Mahakala omnogovae* IGM 100/1033, holotype. (**A**) Right ulna in lateral (right) and medial (left) views. (**B**) Ilium in medial (top) and lateral (bottom) views. (**C**) Femur in posterior (left) and lateral (right) views. (**D**) Tibia in anterior view. (**E**) Left metatarsus in anterior view. (**F**) Right raptorial claw. (**G**) Midcaudal vertebrae. Scale bars, 1 cm in (B) to (E) and 5 mm in (A), (F), and (G). Abbreviations are as follows: aa, ascending process of astragalus; as, astragalus; bf, brevis fossa; brs, brevis shelf; bs, biccipital scar; ca, calcaneum; cc, cnemial crest; ch, chevron; fc, fibular crest; fi, fibula; gtr, greater trochanter; lr, lateral ridge; lc, lateral crest; mco, medial condyle; mt, metatarsal; obr, oblique ridge; pat, posterior antitrochanter; prz, prezygapophysis; pt, posterior trochanter; ts, trochanteric shelf.

to that in *Buitreraptor* (*4*) and *Rahonavis* [UA (University of Antananarivo) 8656]. The chevrons in *Mahakala* are platelike as in many derived coelurosaurs.

The scapula is narrow and straplike and has a strongly compressed ovoid cross section. The preserved portion of the incomplete humerus suggests that the entire humerus was reduced in contrast to the condition of most coelurosaurs. The ulna is distinctly bowed as in most maniraptorans (*1*) but is strongly compressed and possesses a small biceps tubercle. The distal region of the radius is expanded and flattened as in paravians (*11*). A semilunate carpal covers the proximal surfaces of metacarpals I and II; a plesiomorphic conformation lost in most avialans.

The ilium is dolichoiliac. A prominent supratrochanteric process is present as in *Unenlagia*, *Rahonavis*, and many avialans. The brevis shelf is triangular and does not extend laterally as in some other basal dromaeosaurids. No antiliac shelf is present, therefore *Mahakala* lacks a defined cuppedicus fossa—an absence unique within dromaeosaurids but characteristic of avialans such as *Apsaravis* (*15*) and *Yixianornis* (*16*).

The femur is anteriorly bowed. The lesser trochanter is well developed, and its anterior edge is continuous with the greater trochanter. The fourth trochanter is present as a smooth and weakly developed ridge. Unlike *Velociraptor* (IGM 100/986), the lateral ridge is poorly developed, and the moundlike trochanteric shelf is proximodistally elongated and closely connected to the posterior trochanter. A prominent crest extends from the distal third of the shaft to the ectocondylar tubercle. The tibia is longer than the femur and possesses a single cnemial crest. The lateral surface of the calcaneum is distinctly concave and lacks the notch for the articulation with the distal fibula that is present in dromaeosaurids and other nonavian theropods. This condition is shared with *Rahonavis*, basal avialans

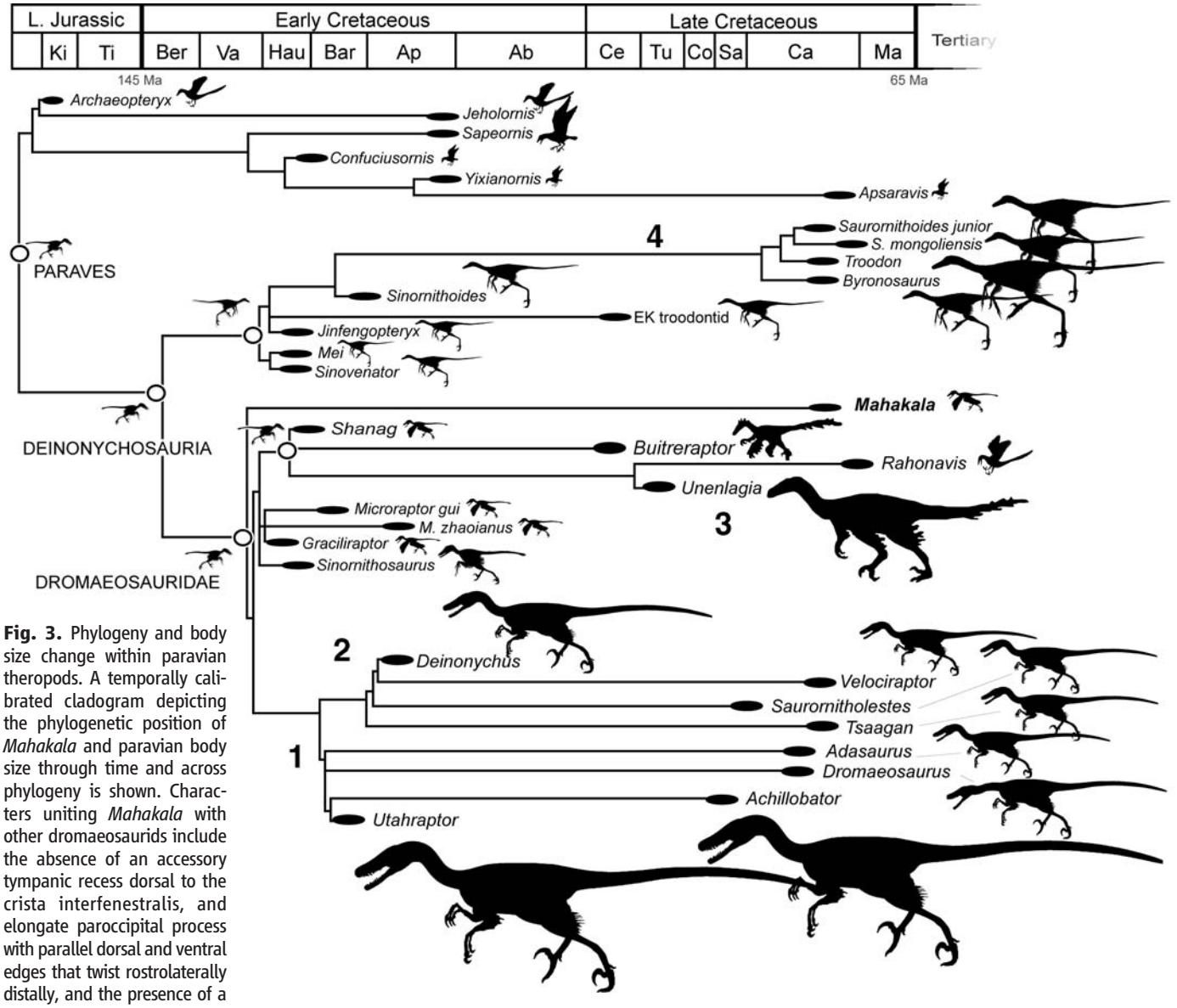

Fig. 3. Phylogeny and body size change within paravian theropods. A temporally calibrated cladogram depicting the phylogenetic position of *Mahakala* and paravian body size through time and across phylogeny is shown. Characters uniting *Mahakala* with other dromaeosaurids include the absence of an accessory tympanic recess dorsal to the crista interfenestralis, and elongate paroccipital process with parallel dorsal and ventral edges that twist rostrolaterally distally, and the presence of a distinct ginglymus on the distal end of metatarsal II (*17*). Silhouettes are to scale, illustrating the relative magnitude of body size differences. Left-facing silhouettes near open circles show reconstructed ancestral body sizes. Ancestral paravian body size is estimated to be 600 to 700 g and 64 to 70 cm long (*17*). The ancestral deinonychosaur, troodontid, and dromaeosaurid body size is estimated at ~700 g. Large numbers (1, 2, 3, and 4) indicate the four major body increase trends in Deinonychosauria. See the supporting online material for further ancestral body size reconstruction data. Ma, Maastrichtian; Ca, Campanian; Sa, Santonian; Co, Coniacian; Tu, Turonian; Ce, Cenomanian; Ab, Albian; Ap, Aptian; Bar, Barremian; Hau, Hauterivian; Va, Valanginian; Ber, Berriasian; Ti, Tithonian; Ki, Kimmeridgian. Ma, million years ago.

(*2*), and derived alvarezsaurids. Unlike most troodontids and microraptorines, but similar to *Archaeopteryx* and derived dromaeosaurids, the foot of *Mahakala* exhibits the plesiomorphic unconstricted condition for metatarsal III, further indicating that this avian trait may be the primitive condition for paravians. The distal end of metatarsal II is composed of an asymmetrical ginglymoid articular surface and phalanx II-2 has a well-developed proximal heel and hypertrophied ginglymoid trochlea. This suite of characters is present only in dromaeosaurids.

Phylogenetic analysis identifies *Mahakala* as a basal dromaeosaurid and supports paravian monophyly with birds (Avialae) as the sister group to a monophyletic Deinonychosauria (Dromaeosauridae + Troodontidae) (Fig. 3 and fig. S1). Although discovered in relatively young Cretaceous deposits, the basal position of *Mahakala* has several implications regarding our understanding of the early history of deinonychosaurians (*17*). First, *Shanag* from the Early Cretaceous of Mongolia (*18*) nests within the purported Gondwanan lineage of dromaeosaurids, Unenlagiinae. This topology complicates recently proposed vicariance-driven origin hypotheses for these groups (*4*, *19*). Second, these dinosaurs are united with Jehol microraptorines (*Microraptor*, *Graciliraptor*, and *Sinornithosaurus*) to form the sister group to derived dromaeosaurids from Laurasia (velociraptorines and allied forms). Third, the purported avialan *Jinfengopteryx* (*20*) is a troodontid. *Jinfengopteryx* has feathers; it thus demonstrates the presence of feathers of modern aspect in a troodontid.

Decrease in body size is a trend in coelurosaurs (*3*, *8*, *21*) and is thought to have played an important role in the origin of birds and flight (*6*, *11*, *22*–*24*). Dromaeosaurids and other coelurosaurs, however, may have undergone clade-specific increases in body size (*8*, *25*). Testing these trends requires empirical size reconstructions for each node of the coelurosaur tree. We estimated ancestral body sizes for each internal node (ancestral node) using body mass estimates from femoral length measurements. These data were treated as a continuous additive trait and optimized across the phylogeny (*16*).

Our analysis (fig. S2) indicates that small body size was not a derived condition at *Archaeopteryx* or Avialae, where flight evolution in theropods is currently inferred. The ancestral dromaeosaurid, troodontid, and deinonychosaurian are reconstructed as small, each with a body mass around 700 g (Fig. 3). The basal members of these lineages are the same size as the early avialan *Jeholornis*. Additionally, our results indicate that deinonychosaurs underwent four parallel trends of body size increase. Three of these events occurred within Dromaeosauridae: *Deinonychus* increased in size by more than two orders of magnitude, as did *Unenlagia,* and the *Achillobator* + *Utahraptor* clade increased by three orders of magnitude. A single trend of body size increase was observed in troodontid body size. These events were contemporaneous with a decrease in avialan body sizes. Our analysis implies that the ancestral paravian had a body size of 600 to 700 g and was ~65 cm long, roughly the size of the largest specimens of *Archaeopteryx* or *Sapeornis* and entailing the size range reconstructed for basal deinonychosaurs. Thus, miniaturization preceded the avialan node and the origin of flight, and as a result, hypotheses relating ontogenetic or metabolic controls on miniaturization to flight origin in theropods must be equally capable of explaining the size reduction within ancestral paravians and the iterative trends of size increase in deinonychosaurs.

References and Notes

1. J. Gauthier, *Mem. Calif. Acad. Sci.* **8**, 1 (1986).
2. C. A. Forster, S. D. Sampson, L. M. Chiappe, D. W. Krause, *Science* **279**, 1915 (1998).
3. P. C. Sereno, *Science* **284**, 2137 (1999).
4. P. J. Makovicky, S. Apesteguía, F. L. Agnolin, *Nature* **437**, 1007 (2005).
5. M. A. Norell *et al*., *Am. Mus. Novit.* **3545**, 1 (2006).
6. X. Xu, Z. Zhou, X.-l. Wang, *Nature* **408**, 705 (2000).
7. X. Xu, M. A. Norell, X.-l. Wang, P. J. Makovicky, X.-C. Wu, *Nature* **415**, 780 (2002).
8. M. A. Norell, X. Xu, *Nature* **431**, 838 (2004).
9. Z. Kielan-Jaworowska, R. Barsbold, *Palaeontol. Pol.* **27**, 5 (1972).
10. D. Dashzeveg *et al*., *Am. Mus. Novit.* **3498**, 1 (2005).
11. M. A. Norell, P. J. Makovicky, *Am. Mus. Novit.* **3282**, 1 (1999).
12. A. Elzanowski, P. Wellnhofer, *Am. J. Sci.* **293**, 235 (1993).
13. P. J. Makovicky, M. A. Norell, in *The Dinosauria,* D. B. Weishampel, P. Dodson, H. Osmólska, Eds. (Univ. of California Press, Berkeley, CA, ed. 2, 2004), pp. 184–195.
14. P. J. Makovicky, M. A. Norell, J. M. Clark, T. Rowe, *Am. Mus. Novit.* **3402**, 1 (2003).
15. M. A. Norell, J. A. Clarke, *Nature* **409**, 181 (2001).
16. J. A. Clarke, Z. Zhou, F. Zhang, *J. Anat.* **208**, 287 (2006).
17. Materials and methods are available as supporting material on *Science* Online.
18. A. H. Turner, S. H. Hwang, M. A. Norell, *Am. Mus. Novit.* **3557**, 1 (2007).
19. F. E. Novas, D. Pol, *Nature* **433**, 858 (2005).
20. Q. Ji *et al*., *Geol. Bull. China* **24**, 197 (2005).
21. M. T. Carrano, in *Amniote Paleobiology: Perspectives on the Evolution of Mammals, Birds, and Reptiles*, M. T. Carrano, T. J. Gaudin, R. W. Blob, J. R. Wible, Eds. (Univ. of Chicago Press, Chicago, 2006), pp. 225–268.
22. Z. Zhou, *Naturwissenschaften* **91**, 455 (2004).
23. E. Buffetaut *et al*., *Naturwissenschaften* **92**, 477 (2005).
24. K. Padian, A. J. de Ricqlés, J. R. Horner, *Nature* **412**, 405 (2001).
25. X. Xu, Q. Tan, X. Zhao, L. Tan, *Nature* **447**, 844 (2007).

26. We thank the field crew of the 1993 field season for their work; X. Xu, Z. Zhou, C. Forster, and D. Krause for specimen access; P. Makovicky, N. Smith, J. Conrad, A. Balanoff, G. Bever, R. Irmis, and S. Nesbitt for discussions; M. Ellison for photographs; and B. Amaral, A. Davidson, and A. Balcarcel for preparation. Support was provided by NSF through a Doctoral Dissertation Improvement Grant (DEB 0608003, presented to A.H.T. and M.A.N.); grant ATOL 0228693 (presented to M.A.N.); the Program in Geoscience, Division of Earth Sciences (grant EAR 0207744, presented to G.M.E. and M.A.N.); and the Division of Biological Infrastructure, Program in Biological Databases and Information (grant DBI 0446224, presented to G.M.E.). Additional support was provided to A.H.T. by the American Museum of Natural History and Columbia University.

Supporting Online Material

www.sciencemag.org/cgi/content/full/317/5843/1378/DC1
SOM Text
Figs. S1 to S5
References

20 April 2007; accepted 30 July 2007
10.1126/science.1144066

20th-Century Industrial Black Carbon Emissions Altered Arctic Climate Forcing

Joseph R. McConnell,[1]* Ross Edwards,[1] Gregory L. Kok,[2] Mark G. Flanner,[3] Charles S. Zender,[3] Eric S. Saltzman,[3] J. Ryan Banta,[1] Daniel R. Pasteris,[1] Megan M. Carter,[4] Jonathan D. W. Kahl[4]

Black carbon (BC) from biomass and fossil fuel combustion alters chemical and physical properties of the atmosphere and snow albedo, yet little is known about its emission or deposition histories. Measurements of BC, vanillic acid, and non–sea-salt sulfur in ice cores indicate that sources and concentrations of BC in Greenland precipitation varied greatly since 1788 as a result of boreal forest fires and industrial activities. Beginning about 1850, industrial emissions resulted in a sevenfold increase in ice-core BC concentrations, with most change occurring in winter. BC concentrations after about 1951 were lower but increasing. At its maximum from 1906 to 1910, estimated surface climate forcing in early summer from BC in Arctic snow was about 3 watts per square meter, which is eight times the typical preindustrial forcing value.

Emissions of black carbon (BC) particles result from incomplete combustion during the burning of biomass and fossil fuels (*1*). In the atmosphere, the absorption of sunlight by BC contributes to global warming and alters cloud-formation processes (*2*). Arctic climate is especially vulnerable to BC deposition because of its impact on the albedo of snow, glaciers, and sea ice—accelerating melting and increasing sensitivity to warming (*3*). Despite its importance, little is known about past natural or anthropogenic emissions of BC and its deposition. Glaciers and ice sheets contain a historical record of atmospheric deposition of aerosol-borne chemicals derived from natural and anthropogenic burning. We used measurements